AMERICAN JOURNAL OF PHYSICAL ANTHROPOLOGY 103:219–233 (1997)

Neandertal Capitate-Metacarpal Articular Morphology

WES A. NIEWOEHNER,[1]* ANNE H. WEAVER,[1]
AND ERIK TRINKAUS[1,2]
[1]*Department of Anthropology, University of New Mexico, Albuquerque, New Mexico 87131*
[2]*URA 376 du C.N.R.S., Laboratoire d'Anthropologie, Université de Bordeaux I, 33405 Talence, France*

KEY WORDS hands; Neandertals; human paleontology

ABSTRACT Neandertal capitate-metacarpal 2 and 3 articulations have been observed to differ in orientation and shape from those of more recent humans. To evaluate this, we tested for differences in capitate-metacarpal 2 (MC2) and MC2-capitate facet orientations and MC2 and MC3 robusticity indices, and for multivariate shape equivalence of the capitate-MC2/MC3 facets and the MC3 diaphysis and styloid process between samples of Neandertals and recent humans. Canonical discriminant functions of log size-and-shape and log shape transformed measurements were run on variables of the capitate-MC2 and MC3 facets, and these plus MC3 diaphysis and styloid process variables.

The null hypothesis of shape equivalence is rejected for both variable sets. Modern human capitate-MC morphology results from nonallometric increases in distal capitate breadth and the projection of the MC3 styloid process, and reductions in MC2 facet height and MC3 facet breadth. These shape changes are associated with a significantly less parasagittal orientation of the capitate-MC2 facets in recent humans, but are only trivially correlated with MC 2 and 3 robusticity indices. The recent human capitate-MC 2 and 3 morphology may reflect a shift in habitual joint reaction forces from more axial to more oblique forces while maintaining similar pronation/supination of the MC2. However, the full behavioral implications of these contrasts remain unclear. Am J Phys Anthropol 103:219–233, 1997.

As the interface between the human organism and the technological substrate upon which (at least) members of the genus *Homo* are dependent, the human hand and its paleontologically documented evolution have attracted paleoanthropological interest since the 19th century. However, most of the focus has been concerned with determining the timing and the paleontological context in which early hominids achieved the level of manual dexterity and precision normally associated with extant humans (e.g., Boule, 1911–13; Napier, 1962; Musgrave, 1971; Marzke, 1983; Ricklan, 1987; Marzke and Marzke, 1987; Lewis, 1989; MacLarnon, 1993; Susman, 1994). From this and related work (e.g., Stoner, 1981; Stoner and Trinkaus, 1981; Heim, 1982; Trinkaus, 1983, 1989; Trinkaus and Villemeur, 1991; Villemeur, 1991), it has become evident that members of the genus *Homo* achieved a level of manual dexterity and (probably) neurological control of the upper limb similar to that of modern humans by the early Late

Contract grant sponsor: N.S.F.; contract grant sponsor: L.S.B. Leakey Foundation; contract grant sponsor: C.N.R.S.; contract grant sponsor: University of New Mexico.

Current address for Erik Trinkaus is Department of Anthropology, Washington University, Campus Box 114, St. Louis, MO 63130.

*Correspondence to: Wes A. Niewoehner, Department of Anthropology, University of New Mexico, Albuquerque, NM 87131. E-mail: wesn@unm.edu

Received 5 October 1995; revised 29 November 1996; accepted 13 March 1997.

Pleistocene, probably in association with the major increase in encephalization which took place during the Middle Pleistocene (Trinkaus 1995; Ruff and Trinkaus, 1996).

While we may conclude that Late Pleistocene archaic humans, such as the European and Near Eastern Neandertals, had achieved manipulative capabilities similar to those of modern humans, mounting evidence from upper limb articular morphology (e.g., Musgrave, 1971; Stoner, 1981; Trinkaus, 1983; Trinkaus and Churchill, 1988; Churchill and Trinkaus, 1990; Trinkaus et al., 1991; Churchill, 1994; Hambücken, 1993; Churchill et al., 1996) indicates that Neandertals may have habitually loaded their upper limb joints at higher levels of joint reaction force and/or in different distributions of articular positions during peak loading. In addition, it has been observed by Riley and Trinkaus (1989; Trinkaus et al., 1991) that the articulations between the capitate and the second and third metacarpals, although similar to those of modern humans in their relative dimensions and articular curvatures, have more parasagittally oriented metacarpal 2 (MC2)-capitate facets and less projecting MC3 styloid processes. From this, they concluded that the Neandertal capitate-MC 2 and 3 articular morphology was not well adapted for resisting oblique joint reaction forces and inferred that the Neandertals did not habitually employ tools which required oblique power grips.

If this interpretation is correct, it would join interpretations of Neandertal shoulder, elbow, and pollical carpo-metacarpal articulations in implying that the Neandertals may well have habitually peak loaded their upper limbs in positions contrasting with those of recent humans, whatever technology they and their early modern human contemporaries and immediate successors were employing. However, the analysis by Riley and Trinkaus (1989) was preliminary, in terms of samples and measurements. We have therefore readdressed this question, testing the null hypothesis of morphological equivalence between the Neandertals and modern humans to assess the presence, magnitude, and nature of morphological (and by extension functional) similarities and differences in this region of manual anatomy.

MATERIALS AND METHODS

Relevant functional morphology

The capitate-metacarpal 2 and 3 articular morphology of modern humans, in contrast with those of the nonhuman Hominoidea, is adapted for resisting and effectively transmitting both axial and oblique (disto-radial to proximo-ulnar) joint reaction forces (Marzke, 1983; Marzke and Marzke, 1987; Lewis, 1989). The former is accomplished by the primary capitate-MC3 facet, which is aligned perpendicular to axial forces (defined by the diaphyseal long axes of the metacarpals) generated by power grips in which the object is held perpendicular to the MC3 diaphyseal axis. The latter is achieved through two smaller facets, the capitate-MC2 facet and the one between the MC3 styloid process and the dorso-disto-radial corner of the capitate. The first facet is obliquely oriented (disto-ulnar to proximo-radial) in the coronal plane of the hand, whereas the latter provides a largely dorso-disto-ulnar to palmar-proximo-radial oriented articular surface. These oblique facets appear to provide resistance to joint reaction forces generated by a variety of power and precision grips which place objects obliquely across the palm and between the pollex and the adjacent two ulnar digits (Napier, 1956; Landsmeer, 1976; Kapandji, 1989).

In addition, whereas there appears to be little movement between the capitate and the MC3, the proximo-ulnarly concave facet between the capitate and the MC2 permits pronation and supination of the MC2, enhancing the opposability of the thumb during precision and oblique power grips (Marzke, 1983). In the possession of this continuous capitate-MC2 facet, all hominids contrast with nonhuman hominoids (Marzke, 1983; McHenry, 1983).

Measurements

To morphometrically assess the variation in these functionally relevant features in Neandertal and recent human capitate, MC2, and MC3 remains, two angles and 10 linear measurements were defined (Table 1, Fig. 1).

The angles describe the orientation of the capitate and MC2 facets. On the capitate,

TABLE 1. Measurements[1,2] for capitate, MC2, and MC3 variables for Neandertals

Specimen	Sex	Variable														
		CMC3Ht	CMC3Br	CapMxBr	CMC2Ht	CMC2Br	CMC2Dp	CMC2A	MC2CA	MC2Len	MC3Len	MC2Ht	MC3Ht	MC2Wd	MC3Wd	StylL
Amud 1[3]	M	11.6	6.9	11.7	13.9	5.7	1.6	50°	—	—	(70.0)	—	8.4	—	7.9	2.0
La Chapelle-aux-Saints[4]	M	14.4	9.3	12.5	12.1	4.7	1.4	54°	—	68.9	(67.0)	9.6	10.5	7.8	8.6	4.0
La Ferrassie 1[4]	M	15.4	9.1	10.1	(13.7)	(3.8)	0.7	75°	17°	68.0	62.0	10.3	8.7	7.4	8.8	1.6
La Ferrassie 2[4,5]	F	11.7	7.6	10.1	(11.4)	4.6	1.4	72°	25°	62.9	59.0	8.4	8.0	6.8	7.7	2.0
Kebara 2[6]	M	16.4	10.5	8.5	12.1	4.6	0.9	56°	8°	68.7	67.9	10.5	9.6	8.5	8.7	3.7
Krapina 200[4]	M[9]	16.4	7.8	11.8	(15.5)	6.2	(1.5)	65°	—	—	—	—	—	—	—	—
Régourdou 1[4]	I[10]	—	—	—	—	—	—	—	39°	63.0	61.6	9.6	9.0	7.9	8.4	4.1
Shanidar 4[4]	M	16.6	11.3	9.4	(12.3)	4.2	0.7	44°	26°	62.8	61.8	9.4	9.4	8.4	8.4	5.0
Shanidar 5[4]	M[9]	—	—	—	—	—	—	—	22°	66.4	—	9.2	—	7.2	—	—
Shanidar 6[4]	F[9]	—	—	—	—	—	—	—	32°	—	57.5	—	8.2	—	7.3	2.6
Spy 1[7]	F[9]	—	—	—	—	—	—	—	14°	—	—	—	—	—	—	—
Spy 2[7]	M[9]	—	—	—	—	—	—	—	15°	62.8	—	9.5	—	8.4	—	—
Tabun 1[8]	F	12.8	9.3	10.5	11.8	3.5	1.2	64°	22°	62.0	(60.8)	8.1	7.6	6.4	6.4	2.2

[1] All variables except CMC2A and MC2CA are in millimeters. Measurements in parentheses are estimates.
[2] See text for variable abbreviations and definitions.
[3] Measurements from casts, Endo and Kimura (1970), and originals.
[4] Measurements from casts and originals.
[5] MC3Len from Heim (1982).
[6] Measurements from originals and cast.
[7] Measurements from casts, Leguebe, personal communication, and originals.
[8] Measurements from casts and originals.
[9] Sex determination based on size.
[10] Sex indeterminate (Vandermeersch and Trinkaus, 1995).

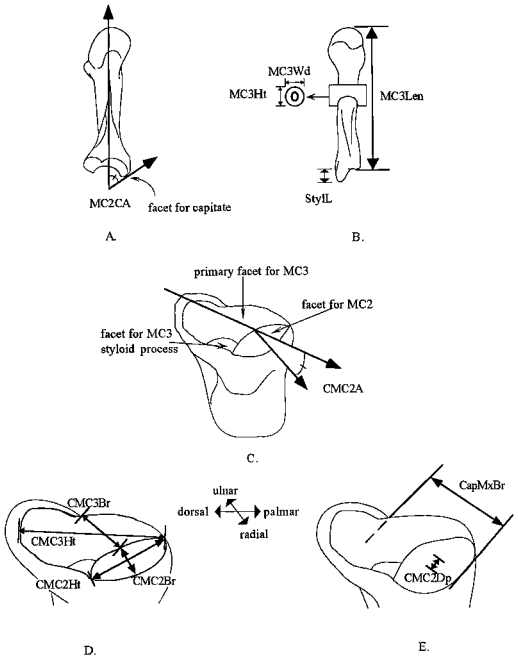

Fig. 1. MC and capitate angles and linear measurements. **A:** Left MC2, palmar view. **B:** Left MC3, dorsal view. **C:** Left capitate, disto-radial view. **D** and **E:** Details of facets for MC2 and MC3 on the distal aspect of the capitate. (Figures not drawn to scale. See text for explanations.)

the MC2 angle (CMC2A) is defined as the angle between the MC2 and MC3 facets, taken in the plane of the capitate at the dorso-palmar midpoint of the MC2 facet; the resultant angles range between 19° and 75°. On the MC2, the capitate angle (MC2CA) is defined as the angle in the coronal plane of the bone (perpendicular to the dorso-palmar axis of the trapezoid facet and including the diaphyseal axis) between the diaphyseal axis and the plane of the capitate facet, taken at the dorso-palmar midpoint of the capitate facet; the resultant angles range between 8° and 75°. These angles were measured with a steel protractor with a moveable arm; repeated measurement on a subset of the recent human sample (n = 25) indicates that intra- and interobserver error is ca. ±1°.

Six linear variables were chosen to describe the size and shape of the MC2 and MC3 facets on the capitate. Additionally, four variables were chosen to describe the size and shape of the MC diaphyses and styloid process. All measurements were taken with digital sliding calipers and, based on repeated measurement of a subsample (n = 25), are considered accurate to ca.0.5 mm.

The set of capitate measurements includes MC3 facet height (CMC3Ht), MC3 facet breadth (CMC3Br), the combined MC2 and MC3 facet breadths (CapMxBr), MC2 facet height (CMC2Ht), MC2 facet depth (CMC2Dp), and MC2 facet breadth (CMC2Br).

CMC3Ht is the maximum dorso-palmar articular height from the most palmar aspect of the junction of the MC2 and MC3 facets to the most dorsal aspect of the articular surface of the MC3 facet. CMC3Br is taken at the midpoint of, and perpendicular to, the dorso-palmar axis of the MC2 facet. CapMxBr is the distance between the most radial aspect of the middle of the MC2 facet to the ulnar margin of the MC3 facet and is perpendicular to the dorso-palmar axis of the MC2 facet.

The dorso-palmar height of the MC2 facet (CMC2Ht) is the chord between the two most distal "peaks" on the facet. This facet is dorso-palmarly concave to flat in both modern human and Neandertal specimens. Usually, this facet has well defined "peaks" that demarcate the dorsal and palmar extents of an evenly concave facet for the MC2; when present, CMC2Ht was taken as the linear distance between these "peaks." However, these sharp peaks are occasionally absent; in these cases, MC2 facet height is measured between the dorsal and palmar points where the curvature of the facet changed from that of being primarily concave to that of being flat. In this manner, CMC2Ht measures the chord of the concavity for the MC2 on the capitate, whether or not there are extensions of the subchondral bone dorsally beyond the actual concavity. In conjunction with this, CMC2Dp is taken as the maximum subtense from the CMC2Ht chord to the facet. CMC2Br is the maximum articular breadth; since the borders of the articular surface approximate an ellipse, its maximum radio-ulnar breadth normally coincides with the midpoint of its dorso-palmar height. The relative curvature of the capitate-MC2 facet is calculated as the ratio of the facet

subtense to its chord (CMC2Dp/CMC2Ht × 100).

The primary MC measurements include the MC3 maximum length (MC3MxLn: proximal styloid process to the most distal point on the head), the articular lengths (MC2/3Len: middle of the carpal articulation to the most distal point on the head [Martin #2 (Bräuer, 1988)]), as well as the midshaft dorso-palmar heights (MC2/3Ht) and radio-ulnar widths (MC2/3Wd) of the diaphysis. The length of the MC3 styloid process (StylL) is derived by subtracting the MC3 articular length from its maximum length.

Robusticity

Although robusticity is often used to describe the relative size of articulations, muscular attachments, or diaphyseal cortical thickness, it is more accurately defined as the strength or rigidity of a structure relative to the mechanically relevant measure of body size (Ruff et al., 1993). In this context robusticity is an important consideration in the functional interpretation of morphological differences since between-sample differences in robusticity (beyond genetically determined minimum requirements) reflect the adaptation to differing levels of mechanical loading, accomplished through the local addition and/or resorption of bone tissue, which must ultimately be transmitted through the articulations. Presumably, between-sample articular morphological contrasts that are significantly correlated with robusticity levels reflect primary adaptations to levels of biomechanical loading transmitted through the diaphyses to the articulations.

With this in mind, robusticity indices ($[MCWd \times MCHt]^{1/2}/MCLEN \times 100$) were computed for both MC2 and MC3. Although scaled cross-sectional parameters provide more accurate measures of the ability of the diaphysis to resist externally applied stresses, external midshaft breadths of ellipsoid diaphyses provide good estimates of the bending and torsional strength of the diaphysis (Ruff, 1990). Metacarpal robusticity indices express the relative average external midshaft diameter, and even though the midshaft breadths are not allometrically scaled to diaphyseal length, these indices should provide a suitable approximation of the relative levels of bending and torsional forces that were habitually resisted in the capitate-MC2/3 region of our samples.

Materials

The fossil samples consist of available capitates and second and third metacarpals from European and Near Eastern Neandertals, deriving from last interglacial and early last glacial (oxygen isotope stages 5 to 3b) deposits. The specimens providing at least one element sufficiently intact to provide relevant measurements, as well as the sufficiently preserved skeletal elements, are indicated in Table 1. Whenever possible, measurements were taken on the original specimens; however, a number of the measurements (as noted in Table 1) were taken on epoxy casts of the whole original specimens (for Amud 1, Régourdou 1, and Shanidar 4, 5 and 6) or one-part epoxy casts of the proximal metacarpal epiphysis or distal capitate (for the remainder of the "cast" measurements); in cases where the capitate facet angle on the MC2 was measured on a proximal epiphyseal cast, it was oriented relative to the diaphyseal axis using the angle in the coronal plane between the trapezoid facet and the diaphyseal axis as measured on the original specimen.

For comparison, the same set of measurements was taken on two samples of recent (late Holocene) humans, including a high activity level late prehistoric horticulturalist Amerindian sample and a modern urban sample (see Ruff et al. [1993] and Churchill [1994] for relative robusticity levels of similar samples).

The late prehistoric Amerindian sample (hereafter referred to as Puebloan) consists of 44 individuals (23 females, 21 males) from the Pueblo IV sites of Kuaua and Pottery Mound in the Maxwell Museum, University of New Mexico. We used standard osteological techniques on cranial and pelvic remains to determine sex. All individuals are from adults (all epiphyses fused) with hand elements lacking signs of osteoarthritis. When possible, we utilized only right capitates and metacarpals, but in 11 cases left capitates and metacarpals had to be used because the right side was missing or damaged. In an additional six cases, at least one of the three

hand elements was from the contralateral side of the same individual. Given this uneven preservation, the actual sample sizes for individual analyses are usually ≤44.

The urban sample of 53 individuals (23 females, 30 males) is from the documented skeletal collection of the Maxwell Museum, University of New Mexico. All are from adults whose hand elements are free from osteoarthritis. The majority of the individuals (n = 47) are of European origin, the remainder are African American (n = 4) and Hispanic (n = 2). Racial affinities are known in some cases; otherwise these determinations are based on standard forensic criteria. All measurements are from the right side.

Data analysis methods

Capitate and MC2 facet angles, MC2/3 robusticity, and capitate-MC2 facet curvature. Since angles are trigonometric transformations of ratios, we initially tested the recent human facet angles and metacarpal robusticity indices for normality with the Shapiro-Wilk statistic (Shapiro and Wilk, 1965). Although distributions for these angles and indices are somewhat skewed and variably kurtotic, none deviate significantly from normality (W = 0.786–0.974). We tested facet angles, MC2/3 robusticity indices, and capitate-MC2 facet curvatures for significant between-sample differences in means with three-way ANOVAs (CMC2A, $P < 0.0001$; MC2CA, $P < 0.0001$; MC2 robusticity, $P = 0.0123$; MC3 robusticity, $P = 0.0072$; facet curvature, $P = 0.999$). We performed pairwise comparisons of sample means with *t*-tests for facet angles and MC2/3 robusticity indices since the ANOVAs indicated significant between-sample differences in means.

Multivariate methods and variable sets. We employed canonical discriminant functions to test the null hypothesis of between-sample morphological equivalence of the capitate-metacarpal 2/3 articulations. This procedure is related to a principle components analysis, but differs in that the canonical discriminant analysis summarizes between-class variance rather than total sample variance. It also produces a number of axes (canonical variates) that have the property of maximizing the ratio of between-group to within-group variability. In general, with K groups there are K−1 discriminant axes possible, although not all of these axes show statistically significant variation across groups. Furthermore, these axes are computed so that the accounted-for variation appears in decreasing order of magnitude (Dillon and Goldstein, 1984).

The multivariate analysis follows the methodology developed by Mossiman and colleagues (Mossiman, 1970; Mossiman and James, 1979; Mossiman and Malley, 1979; Darroch and Mossiman, 1985) in which size and shape are explicitly defined, and then utilized in the interpretation of canonical variates analyses (see also Simmons et al., 1991; Falsetti et al., 1993). Raw data contain information about both "size" and "shape"; therefore, by definition, logged raw variables are log size-and-shape variables. Following Darroch and Mossiman (1985), individual log size is defined as the logged geometric mean of all variables. Shape is the ratio of each variable and the individual's geometric mean. Subtracting the log geometric mean from each logged variable thus creates scale-free shape variables.

Even though log shape variables are a ratio of log size-and-shape and log size variables, log shape and the geometric mean (log size) do not necessarily covary significantly. The empirical relationship between log size and log shape variables is important information concerning the extent to which shape variables are allometric. Significant correlations between shape-transformed variables and the geometric mean indicate allometry; whereas nonsignificant correlations with the geometric mean are indicative of isometry (Mossiman and James, 1979; Simmons et al., 1991; Falsetti et al., 1993).

We divided the specimens into six classes (Neandertal males, Neandertal females, urban males, urban females, Puebloan males, Puebloan females). In order to avoid the problems associated with utilizing data matrices with missing values, we constructed two complete variable sets that maximized the Neandertal sample sizes and performed two separate canonical discriminant functions, 1) the six variables of the capitate (CMC3Ht, CMC3Br, CMC2Ht, CMC2Br,

CMC2Dp, and CapMxBr) and 2) the above six capitate variables plus the four MC3 variables (MC3Ht, MC3Wd, MC3Len, StylL).

The canonical discriminant functions based on the capitate variables have the following class compositions: Neandertal males (n = 6), Neandertal females (n = 2), urban males (n = 30), urban females (n = 23), Puebloan males (n = 20), and Puebloan females (n = 24) (see Table 1 for Neandertal sex-specific sample composition). The canonical discriminant analysis based on the capitate plus MC3 variables has the following class compositions: Neandertal males (n = 5), Neandertal females (n = 2), urban males (n = 30), urban females (n = 23), Puebloan males (n = 16), and Puebloan females (n = 20).

We initially performed principal components analyses on both data sets in order to assess the reductions in total variance after transforming the log size-and-shape variables into log shape variables. Log shape accounts for 70% of the total variance in the capitate variable set and 80% of the total variance in the capitate plus MC3 variable set. This initial analysis indicated the presence of considerable combined sample shape variance that warranted further exploration.

After first testing for homogeneity of within-group covariance matrices following Morrison (1976), discriminant functions were run on log size-and-shape and log shape variable sets. All of the canonical discriminant functions reported utilize pooled within-group covariance matrices and only the canonical axes which display significant between-class variance ($P \leq 0.05$) are discussed. Individuals were then resubstituted back into the discriminant functions and reclassified. The authors recognize that the use of the same data to both construct and evaluate the discriminant functions gives optimistically biased nonerror reclassification rates (Dillon and Goldstein, 1984). Consequently, the reclassification results are used only as a heuristic tool to facilitate the comparison of the log size-and-shape vs. log shape discriminant functions. Finally, we used the distance matrices derived from the discriminant functions of log shape to produce UPGMA clusterings. This allowed us to further evaluate the degree of between-class shape dissimilarities produced by the two variable sets.

RESULTS

Capitate and MC2 angles, MC2/3, robusticity, and capitate-MC2 facet curvature

Neandertals have the lowest mean value for the MC2-capitate facet angle (MC2CA = 22°) and the highest mean value for the capitate-MC2 facet angle (CMC2A = 60°) (Table 2). The Puebloans have intermediate mean values for both facet angles (MC2CA = 44°, CMC2A = 46°, whereas the urban sample has the highest mean MC2CA value (56°) and the lowest mean CMC2A value (39°). Not surprisingly, the two facet angles are significantly inversely correlated (pooled $r = -0.57$, $P < 0.0001$). Additionally, multiple *t*-tests indicate significant differences between all three sample means for both facet angles ($P < 0.0001$ in all cases). However, all three samples have overlapping ranges of variation for both facet angles, the urban and Neandertal samples representing the extreme ranges of variation. Thus, the urban capitate-MC2 and MC2-capitate facets have the most oblique orientations (relative to the coronal plane of the hand), while the Neandertals have the most parasagittally oriented facets.

The Puebloan sample has the lowest mean robusticity indices for both MC2 and MC3 (MC2 = 12.3, MC3 = 12.9) (Table 2). The Neandertal sample has the highest mean MC2 robusticity index (13.0), whereas the urban sample has the highest mean MC3 robusticity index (13.6). Multiple *t*-tests indicate that Neandertal and urban mean MC2 as well as mean MC3 robusticity indices are not significantly different ($P > .05$ in both cases). Differences in mean sample MC2 or MC3 robusticity indices only reach significance ($P \leq .05$) when the Puebloan sample is compared to either the Neandertal (for MC2) or the urban (for MC3) samples. Within samples, mean MC3 robusticity is consistently greater than mean MC2 robusticity, but in no case is mean MC3 robusticity significantly greater than mean MC2 robusticity ($P = 0.82$–0.96).

TABLE 2. Capitate and MC2 angles, MC2/3 robusticity indices, and capitate-MC2 facet curvature

Sample	MC2CA	CMC2A	MC2 robusticity	MC3 robusticity	Capitate-MC2 facet curvature
Neandertal					
n	10	8	9	10	8
Mean	22°	60°	13.0	13.4	9.2
Range	8°–39°	44°–75°	11.6–14.2	11.5–14.4	5.1–11.6
S.D.	9.1°	10.8°	1.0	1.0	2.8
Puebloan					
n	39	41	40	36	41
Mean	44°	46°	12.3	12.9	9.1
Range	21°–59°	31°–58°	10.5–14.3	11.4–14.8	1.9–15.9
S.D.	8.8°	7.0°	1.0	1.0	3.4
Urban					
n	53	53	53	53	53
Mean	56°	39°	12.9	13.6	9.1
Range	30°–75°	19°–58°	10.3–15.2	11.4–16.2	1.2–16.5
S.D.	9.3°	8.9°	1.0	1.0	3.7

The recent human and Neandertal samples have similar values for mean capitate-MC2 facet curvature (Table 2). The slight difference between the deeper average Neandertal capitate-MC2 facet and the slightly flatter average recent human capitate-MC2 facet is not statistically significant.

Multivariate analyses

Capitate variable sets. Table 3 lists the canonical variates of the capitate log size-and-shape variables. Class centroids are plotted on the first two canonical axes with 90% confidence ellipsoids (Fig. 2). The first axis accounts for 66.8% of the total between-class variance. Much of the variance is size related, since the scores along the first axis are significantly correlated with the geometric mean ($r = 0.362$, $P = 0.004$). Separation of the Neandertal and modern human class centroids occurs primarily along the first canonical axis, although the male Neandertal confidence ellipse overlaps with all other modern human class confidence ellipses. Additionally, all of the modern classes have considerable overlap in their confidence regions. A consideration of the variable loadings, plus their correlations with individual scores along the first axis (Table 3), indicates that modern human classes have relatively broader distal capitates (CapMxBr) and dorso-palmarly taller MC3 articular facets (CMC3Ht).

The second axis accounts for 23.7% of the between-class variance and primarily discriminates male and female centroids of each group. The scores along this axis are also highly correlated with the geometric mean ($r = 0.573$, $P \leq 0.001$). All of the variables have positive loadings, and all are significantly correlated with scores along this axis. Therefore, the discriminations along the second axis are also primarily a function of size.

TABLE 3. Canonical variates of capitate log size-and-shape variables

	Canonical coefficients		Correlations between scores and logged variables	
	I[1]	II[1]	I	II
CMC3Ht	0.584	0.803	0.461[2]	0.855[2]
CMC2Ht	−0.297	0.908	−0.147[3]	0.607[2]
CMC2Br	0.287	0.702	0.092[3]	0.302[2]
CMC2Dp	−0.228	0.819	−0.066[3]	0.319[2]
CMC3Br	−0.044	0.747	−0.019[3]	0.459[2]
CapMxBr	0.749	0.503	0.434[2]	0.393[2]

[1] $P < .0001$.
[2] $P \leq .05$.
[3] $P > .05$.

The first canonical axis of the shape transformed capitate variables (Fig. 2) accounts for 83% of the total between-class variance and is the only axis that displays significant between-class variance. The degree of overlap of male and female Neandertal class confidence regions with those of recent humans has increased, indicating the important contribution of size to the previous log size-and-shape discrimination. Scores along the first canonical axis have an extremely low, but significantly non-zero, correlation

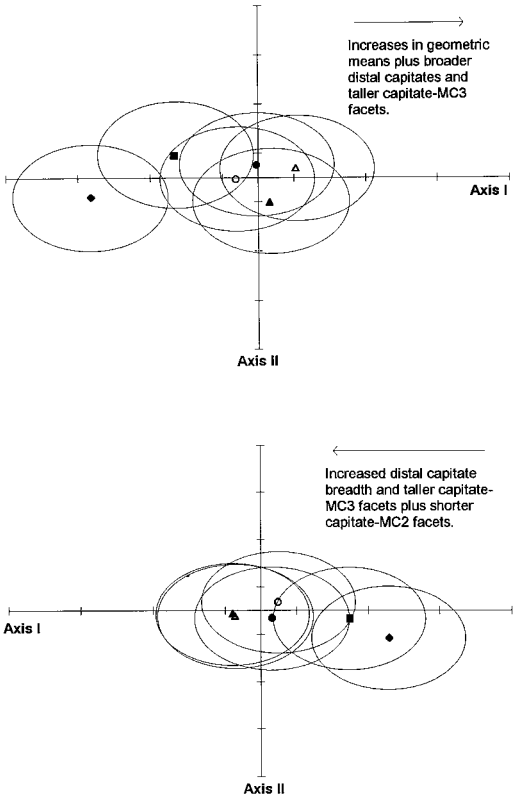

Fig. 2. **Above:** Plot of the canonical discriminant function of log size-and-shape capitate variables. Neandertal and recent human classes are best discriminated along the first axis. This axis accounts for 66.8% of the total between-class variance and individual scores are significantly correlated with geometric means (r = 0.362, $P = 0.004$). **Below:** Plot of the canonical discriminant function of log shape capitate variables. The first axis discriminates Neandertal from recent human classes and accounts for 83% of the total between-class variance. Scores along this axis are not significantly correlated with geometric means (r = 0.192, $P = 0.041$). Class centroids are plotted with 90% confidence ellipses and arrows indicate the nature of significant differences. ■, Neandertal males; ◆, Neandertal females; △, urban males; ▲, urban females; ●, Puebloan males; ○, Puebloan females. See text for further details.

with the geometric mean (r = 0.192, $P = 0.041$), indicating the presence of some residual size in the shape transformed variables. Anatomically modern distal capitates are still distinguished from those of the Neandertals by increases in distal capitate breadth and MC3 facet height but with the addition of a decrease in MC2 facet height (Table 4). Of the three previously mentioned variables, only CMC2Ht is not significantly correlated with the geometric mean.

It is possible that allometric shape changes contribute significantly to the discrimination of Neandertal distal capitates from those of the recent human classes since CapMxBr and CMC3Ht are both significantly correlated with the geometric mean. If this is true, the largest capitates (those with larger geometric means) should have the shortest capitate-MC3 facets and the most narrow distal capitates, since both variables (CMC3Ht and CapMxBr) have negative correlations with the geometric mean (Table 4).

On average, Puebloan females have the smallest distal capitates (class geometric mean = 1.096), followed by Neandertal females (1.106), urban females (1.107), Puebloan males (1.139), urban males (1.145), and Neandertal males (1.152). An inspection of the capitate shape variables discriminant function (Fig. 2) reveals that class means along the first axis are not positioned with respect to the predicted allometric relationship between geometric mean and distal capitate shape. The small Puebloan females should fall to the far left of the first canonical axis, with allometrically wide distal capitates and tall MC3 facets, while the large Neandertal and urban males should be at the far right of the first axis with narrow distal capitates and short MC3 facets. Additionally, if allometry had a significant effect on this discriminant function, the Neandertal females should be more similar to the recent human females than to the Neandertal males.

Similarly, the orientation of the capitate-MC2 facet could be an allometric effect of capitate size if the capitate-MC2 facet angle were significantly correlated with the geometric mean. However, the capitate-MC2 angle is not significantly correlated with the geometric mean (pooled r = 0.070, $P = 0.483$; with class means, r = 0.348, $P = 0.516$). Therefore allometry, although present, does not have a significant effect on this shape discriminant function.

Capitate plus MC3 variable sets. The first canonical axis of log size-and-shape capitate plus MC3 variables (Fig. 3) accounts for 47.9% of between-class variance, and discriminates males from females of the same group. Most of the variance is size

TABLE 4. Canonical variates of capitate log shape variables

	Canonical coefficients		Correlation between scores and shape variables		Correlation between shape variables and geometric mean
	I[1]	II[2]	I	II	
CMC3Ht	−0.763	0.616	−0.265[3]	0.491[3]	−0.793[1]
CMC2Ht	0.882	−0.067	0.411[3]	−0.072[4]	−0.157[4]
CMC2Br	−0.279	0.698	−0.113[4]	0.651[3]	−0.209[3]
CMC2Dp	0.597	−0.293	0.153[4]	−0.173[4]	0.758[1]
CMC3Br	0.237	−0.852	0.046[4]	−0.381[3]	−0.529[1]
CapMxBr	−0.928	−0.137	−0.460[3]	−0.156[4]	−0.626[1]

[1] $P < .0001$.
[2] $P = .2498$.
[3] $P \leq .05$.
[4] $P > .05$.

related, since individual scores along this axis are significantly correlated with the geometric mean ($r = 0.551$, $P < 0.0001$) and all variables that have significant correlations with their scores along this axis have positive loadings (Table 5).

The second canonical axis accounts for 35.2% of the total between-class variance and discriminates the modern human classes from the Neandertal ones. Neandertal and recent human confidence regions now have less overlap than was apparent in the discriminant functions based on capitate variables (Fig. 2). Individual scores are not significantly correlated with the geometric mean ($r = 0.106$, $P = 0.300$), indicating that between-class variance along this axis is primarily a function of shape. Recent human centroids are maximally separated from the Neandertal centroids by an increase in the projection of the MC3 styloid process (StylL) contrasted with decreases in MC3 facet breadth, MC2 facet height, and the length and width of the MC3 diaphysis (Table 5).

The first canonical axis of the capitate plus MC3 log shape variables accounts for 57.3% of the between-class variance, and the second axis accounts for 31.2% of the between-class variance. Individual scores along the first and second axes are not significantly correlated with log size (axis I, $r = -0.122$, $P = 0.235$; axis II, $r = 0.150$, $P = 0.144$). The Neandertal centroids are separated from the modern ones primarily along the first canonical axis, although with a slight increase in the degree of overlap in confidence regions due to the reduction in between-class size variance. The modern human centroids remain distinguished from

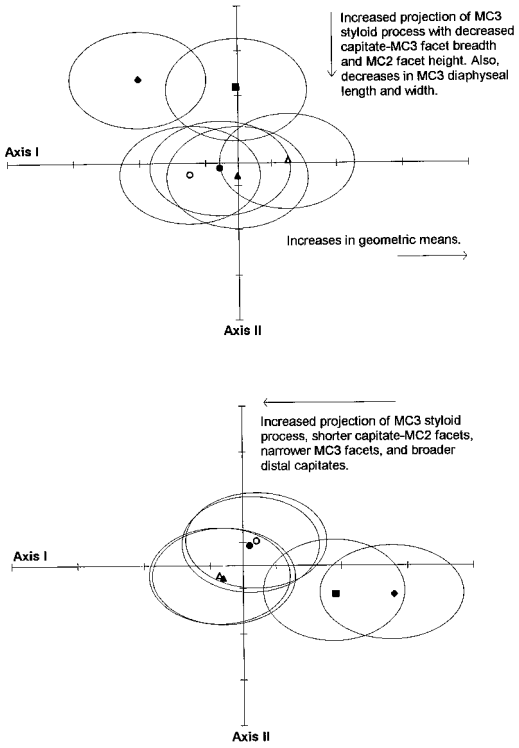

Fig. 3. **Above:** Plot of the canonical discriminant function of log size-and-shape capitate plus MC3 variables. Neandertal and recent human classes are best discriminated along the second axis. This axis accounts for 35.2% of the total between-class variance and individual scores are not significantly correlated with geometric means ($r = 0.106$, $P = 0.300$). **Below:** Plot of the canonical discriminant function of log shape capitate plus MC3 variables. The first axis discriminates Neandertal from recent human classes and accounts for 57.3% of the total between-class variance. Scores along this axis are not significantly correlated with geometric means ($r = -0.122$, $P = 0.235$). Class centroids are plotted with 90% confidence ellipses and arrows indicate the nature of significant morphological differences. ■, Neandertal males; ◆, Neandertal females; △, urban males; ▲, urban females; ●, Puebloan males; ○, Puebloan females. See text for further details.

TABLE 5. Canonical variates of capitate and MC3 log size-and-shape variables

	Canonical coefficients		Correlations between scores and logged variables	
	I[1]	II[1]	I	II
CMC3Ht	0.556	−0.205	0.423[2]	−0.166[3]
CMC2Ht	0.084	0.634	0.041[3]	0.329[2]
CMC2Br	0.134	−0.484	0.033[3]	−0.126[3]
CMC2Dp	−0.039	0.430	−0.012[3]	0.147[3]
CMC3Br	0.490	0.706	0.235[2]	0.362[2]
CapMxBr	0.917	−0.066	0.501[2]	−0.039[3]
MC3Ht	0.928	0.311	0.751[2]	0.269[3]
MC3Wd	0.934	0.346	0.821[2]	0.325[2]
MC3Len	0.874	0.458	0.640[2]	0.359[2]
StylL	0.563	−0.759	0.267[2]	−0.385[2]

[1] $P < .0001$.
[2] $P \leq .05$.
[3] $P > .05$.

those of the Neandertals by their longer MC3 styloid processes, dorso-palmarly shorter MC2 facets, and radio-ulnarly narrower MC3 facets, but also by their radio-ulnarly expanded distal capitates (Table 6). The MC3 diaphyseal variables are no longer significantly correlated with scores along this axis, and none of these shape variables retain significant correlations with the geometric mean.

The capitate-MC2 facet angle (CMC2A) is significantly correlated with individual scores along the first axis, but not the second axis, of both log shape discriminant functions ($r = 0.687$ for log shape capitate variables; $r = -0.648$, for log shape capitate plus MC3 variables [Table 7]). If we use class means for this angle, the correlation with mean scores along the first axis of both shape discriminant functions increases dramatically. For example, the correlation between mean CMC2A values and the first shape axis of capitate shape variables is 0.994 and 0.996 for capitate plus and MC3 shape variables. Correlations with the second axes are not significant. This is, not surprisingly, associated with similarly high (and significant) correlations between the individual and mean MC2CA values and the first shape axis of capitate and capitate plus MC3 shape variables (Table 7).

Metacarpal 3 diaphyseal variables have high and significant loadings on the second axis of capitate plus MC3 shape variables (Table 6). Not surprisingly, pooled sample MC3 robusticity indices also have the highest correlations with both class means and individual scores on this axis (Table 7). Metacarpal 2 robusticity indices are also correlated with scores along this axis, but this is due to the fact that MC2 and MC3 robusticity indices are themselves highly correlated ($r = 0.769$ $P \leq 0.0001$). More important than the previous correlations is the fact that MC3 robusticity indices retain significant, albeit low, correlations with the second shape axis of the capitate shape variables, even though MC3 diaphyseal variables were not used in this discriminant function.

This pattern of correlations indicates that if there is any effect of robusticity on capitate shape, it is most likely to occur along variation in the second rather than the first shape axis of both discriminant functions. An inspection of the variable loadings on both of these axes (Table 4, axis II; Table 6, axis II) indicates that increases in metacarpal robusticity covaries with relative decreases in capitate-MC3 facet height and capitate-MC2 facet breadth. However, these shape differences do not appear to be an important discriminator of Neandertals from recent humans since the second axis of capitate shape variables has insignificant between-class variance (Fig. 2, Table 4) and Neandertal and recent human classes are not discriminated along the second axis of capitate plus MC3 shape variables (Fig. 3, Table 6).

The results of the resubstitution of individuals back into the discriminant functions are summarized in Table 8. None of the Neandertals are misclassified into the recent human classes when both log size-and-shape and log-shape variables of the capitate plus MC3 are used. Although all four discriminant functions reclassify modern individuals as Neandertals, the capitate plus MC3 variable set has lower error rates than the capitate variable set alone, reflecting the inclusion of the MC3 styloid process in the second data set. The use of log shape variables of the capitate and MC3, vs. log size-and-shape variables, results in a small increase in the error rate of the reclassification of modern humans, possibly indicating some

TABLE 6. Canonical variates of capitate and MC3 log shape variables

	Canonical coefficients		Correlation between scores and shape variables		Correlation between shape variables and geometric mean
	I[1]	II[2]	I	II	
CMC3Ht	−0.446	0.842	−0.194[4]	0.432[3]	−0.451[3]
CMC2Ht	0.909	0.284	0.510[3]	0.187[4]	0.010[4]
CMC2Br	−0.011	0.760	−0.005[4]	0.361[3]	0.194[4]
CMC2Dp	0.598	0.400	0.196[4]	0.154[4]	0.482[1]
CMC3Br	0.769	−0.456	0.273[3]	−0.189[4]	−0.189[4]
CapMxBr	−0.825	−0.407	−0.292[3]	−0.169[4]	−0.083[4]
MC3Ht	−0.244	−0.902	−0.132[4]	−0.575[3]	−0.107[4]
MC3Wd	−0.164	−0.966	−0.106[4]	−0.731[3]	−0.292[3]
MC3Len	0.278	−0.799	0.107[4]	−0.362[3]	−0.473[1]
StylL	−0.869	0.125	−0.416[3]	0.070[4]	−0.115[4]

[1] $P < .0001$.
[2] $P = .0006$.
[3] $P \leq .05$.
[4] $P > .05$.

TABLE 7. Correlations between capitate angle, MC2 angle, and MC2/3 robusticity with canonical shape axes scores

	Capitate shape variables		Capitate + MC3 shape variables	
	Axis I r	Axis II r	Axis I r	Axis II r
Class means				
MC2 robusticity	0.073[3]	−0.240[3]	0.066[3]	−0.610[3]
MC3 robusticity	−0.047[3]	−0.285[3]	−0.036[3]	−0.612[3]
CMC2A	0.994[1]	−0.725[3]	0.996[1]	−0.503[3]
MC2CA	−0.979[1]	0.588[3]	−0.955[2]	0.487[3]
Total sample				
MC2 robusticity	−0.099[3]	−0.204[2]	−0.215[2]	−0.256[2]
MC3 robusticity	−0.126[3]	−0.247[2]	−0.262[1]	−0.419[1]
CMC2A	0.687[1]	−0.023[3]	0.648[1]	−0.146[3]
MC2CA	−0.580[1]	0.000[3]	−0.558[1]	0.153[3]

[1] $P \leq .0001$.
[2] $P \leq .05$.
[3] $P > .05$.

TABLE 8. Resubstitution summaries for discriminant functions

	Percent incorrect reclassification	
	Neandertals as recent humans[1]	Recent humans[1] as Neandertals
Capitate variables		
Log size-and-shape	12.5	4.1
Log shape	12.5	5.1
Capitate and MC3 variables		
Log size-and-shape	0.0	1.0
Log shape	0.0	2.0

[1] Includes all recent human classes.

residual influence of size on the quality of the discriminant function.

A comparison of the two trees derived from UPGMA clusterings of log shape variable sets (Fig. 4) indicates that they produce identical hierarchical clusterings of Neandertal and modern human classes. The Puebloan and urban centroids form one cluster, with males and females of the same group having the smallest branch lengths. Neandertals are separated from the modern clusters by long branch lengths in both figures. However, the UPGMA cluster produced from the capitate plus MC3 log-shape variable set has a longer branch length between the Neandertal and recent human classes than does the cluster based on log shape capitate variables. This further reinforces the conclusion that the inclusion of the MC3 styloid process in the second variable set increases the quality of the discriminant function.

DISCUSSION

Our univariate and multivariate analyses confirm Riley and Trinkaus' (1989) conclu-

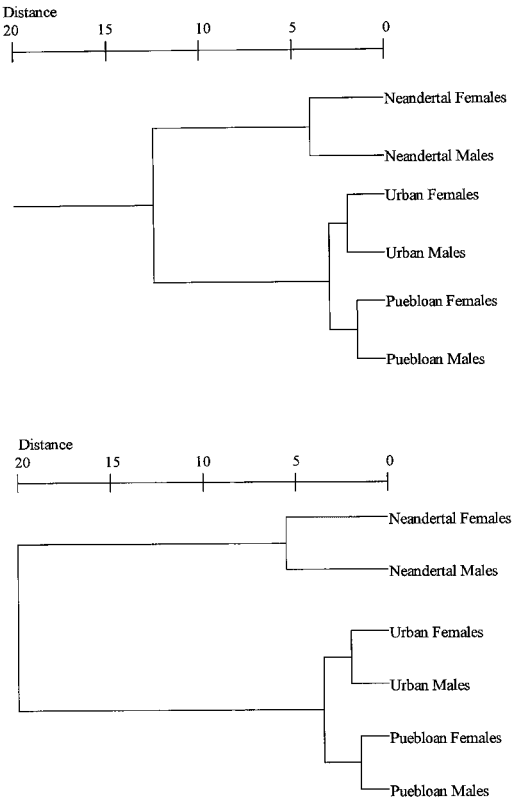

Fig. 4. **Above:** Results of UPGMA analysis utilizing log shape capitate variables. **Below:** Results of UPGMA analysis utilizing log shape capitate plus MC3 variables. Neandertals are separated from recent human classes by long branch lengths in both trees but the cluster produced from the capitate plus MC3 log-shape variables has the longer branch. This indicates that the inclusion of the MC3 styloid process in the discriminant function increases its discriminatory power.

sion of a significant reorientation of the MC2 facet in the coronal plane from parasagittal to oblique between Neandertals and recent humans, accompanied by significantly increased projection of the MC3 styloid process. We have also identified correlated shape changes in the recent human capitate-MC2/3 articulations, which include a combination of dorso-palmarly shorter capitate-MC2 facets, radio-ulnarly narrower capitate-MC3 facets, and radio-ulnarly broader distal capitates. Notably, these articular shape changes are nonallometric and therefore cannot be adequately explained through the effects of size on articular shape.

This analysis was not designed specifically to test the assertion that these morphological differences are primary adaptations to frequency shifts in the use of transverse vs. oblique power grips, as suggested by Riley and Trinkaus (1989). Yet it does establish the fact that Neandertal and recent human capitate-MC2/3 articulations have significant, functionally relevant morphological contrasts. This is important, even though their behavioral correlates remain uncertain.

Although the orientation and shape of the recent human capitate-MC2/3 articulations have changed, Neandertals and recent humans probably maintained functional equivalence with respect to the ability of the MC2 to pronate. As previously noted, the proximo-ulnar concavity of the MC2 facet on the capitate permits some degree of pronation/supination of the MC2 which aids in the opposition of the thumb against the index finger. In the relative concavity of the capitate-MC2 facet, Neandertals and recent humans do not differ since our data indicate nonsignificant differences in between-sample mean capitate-MC2 facet curvatures. However, also facilitating this movement in recent humans is the lack of an interosseous MC2/3 ligament and a transversely oriented trapezium-MC2 facet (Lewis, 1989). There are no indications of a Neandertal interosseous ligament, and the orientations of their trapezial-MC2 facets, although qualitatively similar to those of recent humans, have not yet been quantified. Thus, assuming no significant differences in the orientation of the trapezial-MC2 facet, Neandertals appear to have had sufficiently mobile second metacarpals to have no restrictions of their ability to oppose the index finger and thumb.

The proximal elongation of the recent human MC3 styloid process increases the contact area between the base of the MC3 and the dorso-disto-radial corner of the capitate, more effectively limiting the palmar and ulnar movement of the MC3 base. Combined with a more distally oriented capitate-MC2 facet, this provides more effective transmission of oblique joint reaction forces (Marzke and Marzke, 1987). Given these important functions, the interpretation that the recent human capitate-MC2/3 region is better adapted to the effective transmission of both oblique and axial forces cannot be

discounted. However, it is also apparent that the recent human distal capitate has undergone a more substantial remodeling than was previously thought, and it remains to be determined whether nearby functional complexes, such as the MC2-trapezoid articulation, have undergone associated remodeling.

Most Neandertal upper limb attachment areas indicate heavily muscled forearms and hands (Trinkaus, 1983; Stoner, 1981; Churchill and Trinkaus, 1990; Villemeur, 1991). The large crest for the insertion of *M. opponens pollicis* on Neandertal first metacarpals and the presence of a crest for the insertion of the *M. opponens digiti minimi* on most fifth metacarpals, as well as their large trapezium and hamate tubercles, are all evidence of their hypertrophied thenar and hypothenar musculature (Trinkaus, 1983; Vandermeersch, 1991). Consequently, relatively high joint reaction forces could have been generated on the radial and ulnar aspects of the hand during powerful gripping behaviors. The dorso-palmarly flat Neandertal CMC1 articulation is likely to be an adaptation to such forces, since it would have more effectively transmitted these higher levels of joint reaction force than the recent human CMC 1 articulation (Trinkaus, 1989).

There is less convincing evidence that the Neandertal capitate-MC2/3 region experienced similarly high levels of biomechanical forces. Neandertal second and third metacarpals are not significantly more robust than those of the Urban comparative sample, indicating that both samples were probably subjected to similar levels of biomechanical forces in this region of the hand. The low correlations between metacarpal robusticity and the shape vectors that discriminate recent human and Neandertal capitate-MC articulations (Table 7) indicate that robusticity has a trivial effect on those aspects of distal capitate morphology. This conclusion is also buttressed by the fact that, despite having significantly lower metacarpal robusticity indices than both the urban and Neandertal samples, the Puebloan sample is morphologically most similar to the urban sample. Thus, the shift from Neandertal to recent human capitate-MC2/3 morphology is probably not related to altered levels of habitual biomechanical force transmission.

CONCLUSIONS

Given the lack of evidence for substantial adaptations to differences in the levels of biomechanical forces habitually transmitted, an alternative functional explanation that the Neandertal-recent human capitate-metacarpal 2/3 articular orientation and shape contrasts are primarily the product of adaptations to significantly altered force vectors remains a viable hypothesis to be tested further. Importantly, it now appears likely that some between-sample contrasts of Neandertal articular anatomy, such as the shape of the CMC1 articulation, are primary responses to changing articular load levels, whereas other morphological contrasts, such as those investigated here, are primary responses to altered force vectors.

ACKNOWLEDGMENTS

We thank H. Duday for calling our attention to the exceptional parasagittal orientation of the Kebara 2 MC2 capitate facet, T. Kimura, A. Langaney, A. Leguebe, Muayed Saiid al-Damirji, R. Orban, J. Radovčić, R. Saban, M. Soubeyran, C.B. Stringer, B. Vandermeersch, and J. Zias for access to human fossil remains used in this study, and J.S. Rhine and J.F. Powell for permission to use the Maxwell Museum skeletal collections.

LITERATURE CITED

Boule M (1911–13) L'homme fossile de La Chapelle-aux-Saints. Ann. Paléontol. *6:*111–172; *7:*21–56, 85–192; *8:*1–70.

Bräuer G (1988) Osteometrie. In R Knuβmann (ed.): Wesen und Methoden der Anthropologie. Stuttgart: Gustav Fischer Verlag, vol. 1, pp. 160–232.

Churchill SE (1994) Human upper body evolution in the Eurasian Upper Pleistocene. PhD dissertation, University of New Mexico.

Churchill SE and Trinkaus E (1990) Neandertal scapular glenoid morphology. Am. J. Phys. Anthropol. *83:* 147–160.

Churchill SE, Pearson O, Grine FE, Trinkaus E, and Holliday TW (1996) Morphological affinities of the proximal ulna from Klasies River main site: Archaic or modern? J. Hum. Evol. *31:*213–237.

Darroch JN and Mossiman JE (1985) Canonical and principal components of shape. Biometrika *72:*241–252.

Dillon WR and Goldstein M (1984) Multivariate Analysis: Methods and Applications. New York: Wiley and Sons.

Endo B and Kimura T (1970) Postcranial skeleton of the Amud man. In H Suzuki and F Takai (eds.): The Amud

Man and His Cave Site. Tokyo: Academic, pp. 231–406.
Falsetti AB, Jungers W, and Cole T (1993) Morphometrics of the Callithricid forelimb: A case study in size and shape. Int. J. Primatol. *14:*551–571.
Hambücken A (1993) Variabilité morphologique et metrique de l'humérus, du radius et de l'ulna des néandertaliens. Comparisons avec l'homme moderne. Thèse de doctorat, Université de Bordeaux I.
Heim JL (1982) Les hommes fossiles de La Ferrassie II. Arch. Inst. Paléontol. Hum. *38:*1–272.
Kapandji AI (1989) La préhension dans la main humaine. Ann. Chir. Main *8:*234–241.
Landsmeer JMF (1976) Atlas of Anatomy of the Hand. Edinburgh: Churchill Livingstone.
Lewis OJ (1989) Functional Morphology of the Evolving Hand and Foot. Oxford: Oxford University Press.
MacLarnon A (1993) The vertebral canal. In A Walker and R Leakey (eds.): The Nariokotome *Homo erectus* Skeleton. Cambridge: Harvard University Press, pp. 359–390.
Marzke MW (1983) Joint functions and grips of the *Australopithecus afarensis* hand, with special reference to the region of the capitate. J. Hum. Evol. *12:*197–211.
Marzke MW and Marzke RF (1987) The third metacarpal styloid process in humans: Origins and functions. Am. J. Phys. Anthropol. *73:*415–431.
McHenry HM (1983) The capitate of *Australopithecus afarensis* and *A. africanus.* Am. J. Phys. Anthropol. *62:*187–198.
Morrison DF (1976) Multivariate Statistical Methods, 2nd ed. New York: McGraw-Hill.
Mossiman JE (1970) Size allometry: Size and shape variables with characterizations of the lognormal and generalized gamma distributions. J. Am. Statist. Assoc. *56:*930–945.
Mossiman JE and James FC (1979) New statistical methods for allometry with application to Florida red-winged blackbirds. Evolution *33:*444–459.
Mossiman JE and Malley JD (1979) Size and shape variables. In L Orloci, CR Rao, and WM Stiteler (eds.): Multivariate Methods in Ecological Work. Burtonsville, Md.: Int. Coop., pp. 175–189.
Musgrave JH (1971) How dextrous was Neanderthal man? Nature *233:*538–541.
Napier JR (1956) The prehensile movements of the human hand. J. Bone Joint Surg. *38B:*902–913.
Napier JR (1962) Fossil hand bones from Olduvai Gorge. Nature *196:*409–411.
Ricklan DE (1987) Functional anatomy of the hand of *Australopithecus africanus.* J. Hum. Evol. *16:*643–664.
Riley K and Trinkaus E (1989) Neandertal capitate-metacarpal 2 articular morphology and Neandertal manipulative behavior (abstract). Am. J. Phys. Anthropol. *78:*290.
Ruff CB (1990) Body mass and hindlimb bone cross-sectional and articular dimensions in anthropoid primates. In J Damuth and BJ McFadden (eds.): Body Size in Mammalian Paleobiology: Estimation and Biological Implications. Cambridge: Cambridge University Press, pp. 119–149.
Ruff CB and Trinkaus E (1996) Body mass in Pleistocene *Homo* (abstract). Am. J. Phys. Anthropol. Suppl. *22:* 205.
Ruff CB, Trinkaus E, Walker A, and Larsen CS (1993) Postcranial robusticity in *Homo.* I: Temporal trends and mechanical interpretations. Am. J. Phys. Anthropol. *91:*21–53.
Shapiro SS and Wilk MB (1965) An analysis of variance test for normality (complete samples). Biometrika *52:*591–611.
Simmons T, Falsetti AB, and Smith FS (1991) Frontal bone morphometrics of southwest Asian Pleistocene hominids. J. Hum. Evol. *20:*249–269.
Stoner BP (1981) A statistical analysis of the Neanderthal thumb: Functional adaptations for the transmission of force. BA thesis, Harvard University.
Stoner BP and Trinkaus E (1981) Getting a grip on Neandertals: Were they all thumbs? (abstract) Am. J. Phys. Anthropol. *54:*281–282.
Susman RL (1994) Fossil evidence for early hominid tool use. Science *265:*1570–1573.
Trinkaus E (1983) The Shanidar Neandertals. New York: Academic.
Trinkaus E (1989) Olduvai Hominid 7 trapezial metacarpal 1 articular morphology: Contrasts with recent humans. Am. J. Phys. Anthropol. *80:*411–416.
Trinkaus E (1995) Brains and bodies: Mosaic trends in Middle Pleistocene archaic *Homo* morphology. In JM Bermúdez de Castro, JL Arsuaga, and E Carbonell (eds.): Evolución Humana en Europa y los Yacimientos de la Sierra de Atapuerca. Valladolid: Consejería de Cultura y Turismo, Junta de Castilla y León. *1:*205–228.
Trinkaus E and Churchill SE (1988) Neandertal radial tuberosity orientation. Am. J. Phys. Anthropol. *75:* 15–21.
Trinkaus E and Villemeur I (1991) Mechanical advantages of the Neandertal thumb in flexion: A test of an hypothesis. Am. J. Phys. Anthropol. *84:*249–260.
Trinkaus E, Churchill SE, Villemeur I, Riley KG, Heller JA, and Ruff CB (1991) Robusticity *versus* shape: The functional interpretation of Neandertal appendicular morphology. J. Anthropol. Soc. Nippon *99:*257–278.
Vandermeersch B (1991) La ceinture scapulaires et les membres supérieurs. In O Bar-Yosef and B Vandermeersch (eds.): Le Squelette Moustérien de Kébara 2. Paris: C.N.R.S., pp. 157–178.
Vandermeersch B and Trinkaus E (1995) The postcranial remains of the Régourdou 1 Neandertal: The shoulder and arm remains. J. Hum. Evol. *28:*439–476.
Villemeur I (1991) Etude morphologique et biomécha-nique du squelette de la main des Néandertaliens, comparison avec la main des hommes actuels. Thèse doctorat, Université Bordeaux I.